Available online at www.sciencedirect.com
SCIENCE DIRECT
Journal of Catalysis 229 (2005) 105–113
JOURNAL OF CATALYSIS
www.elsevier.com/locate/jcat

Rearrangement of allyl phenyl ether over Al-MCM-41

Nevin T. Mathew, S. Khaire, S. Mayadevi, R. Jha, S. Sivasanker *

National Chemical Laboratory, Pune 411008, India

Received 13 July 2004; revised 29 September 2004; accepted 30 September 2004

Available online 24 November 2004

Abstract

Claisen rearrangement of allyl phenyl ether to *o*-allylphenol and a dihydrobenzofuran derivative was investigated over MCM-41 with different Si/Al ratios. Higher aluminum content, higher reaction temperatures, and longer run duration favor the formation of the ring compound 2,3-dihydro-2-methyl benzofuran. There is a close relationship between acidity and conversion, which suggests that the reaction occurs inside the large pores of MCM-41. The influence of temperature and catalyst Si/Al ratio on the reaction are examined by kinetic analysis, under the assumption of a first-order consecutive reaction.

Keywords: Claisen rearrangement; Allyl phenyl ether; Al-MCM-41; Molecular rearrangement; Solid acids; Mesoporous material

1. Introduction

Claisen rearrangement involves the conversion of allyl phenyl ethers (APEs) to the corresponding *o*-allylphenols and is generally performed by heating the ethers at an elevated temperature (> 473 K), but has been reported to be susceptible to catalysis by Lewis and Brønsted acids [1,2]. Reports of the use of solid acids in the above rearrangement are rather scarce. Pitchumani et al. have observed shape selectivity in ZSM-5 and ZSM-11 during their study of photo-assisted Claisen rearrangement [3]. Sheldon et al. have investigated the use of H-FAU and H-MOR in the rearrangement of APE in benzene medium [4,5]. Other solid catalysts that have been investigated are mesoporous silica [6] and bentonite [7]. We have already reported our studies on the use of large-pore zeolites, especially beta, as catalysts for the rearrangement [8]. As we did not find any meaningful relationship between acidity and catalytic activity in these zeolites, we suggested that even over large-pore zeolites, the rearrangement occurs primarily at the external surface or at the pore mouth [8].

Mesoporous molecular sieves of the MCM-41 type have received much attention because of their large surface area and the uniform size and shape of the pores over micrometer-length scales [9,10]. High thermal stability and the advantage of tuning the pore size make these materials interesting for use as supports and catalysts for various heterogeneously catalyzed reactions. In the present study, we have explored the use of Al-MCM-41 with large pores (∼ 30-Å diameter) as a catalyst in the Claisen rearrangement of APE. The effect of reaction parameters and catalyst Al content on conversion and product selectivity has been studied. A kinetic analysis of the formation of the different products under various reaction conditions is also presented.

2. Experimental

Tetraethyl orthosilicate (Aldrich), aluminum sulfate (s.d. fine chemicals Ltd.), cetyltrimethylammonium bromide (CTMABr) (Loba Chemie), and tetramethylammonium hydroxide (TMAOH) (Aldrich) were used in the synthesis of the samples. Si-MCM-41 was prepared hydrothermally in alkaline medium with the use of a gel with the molar composition 1 SiO_2:0.33 TMAOH:0.55 CTMABr:60 H_2O.

* Corresponding author. Fax: +91 20 2589 3761.
E-mail address: siva@cata.ncl.res.in (S. Sivasanker).

0021-9517/$ – see front matter
doi:10.1016/j.jcat.2004.09.027

Al-MCM-41 with different Si/Al ratios was prepared by the addition of aluminum sulfate to the Si-MCM-41 gel to get the molar composition 1 SiO_2:0.33 TMAOH:0.55 CTMABr:60 H_2O:x Al_2O_3. Al-MCM-41 with Si/Al ratios of 20, 30, 50, and 100 was prepared by the variation of x in the gel composition from 0.005 to 0.025 moles. In all cases, the gel was aged at room temperature for 5 h with stirring and heated in an autoclave at 383 K for 5 days under autogenous pressure. The solid product was filtered, washed, dried, and calcined at 823 K for 8 h to get the final product. The product was characterized by X-ray diffraction (XRD) (Rigaku D/MINI-Flex X-ray diffractometer, 40 kV, 20 mA, Ni filtered Cu-K_α), scanning electron microscopy (JEOL JSM 5200), nuclear magnetic resonance (Brucker MSL-300), and N_2 adsorption. The samples were characterized for their acidity by the temperature-programmed desorption (TPD) of NH_3 (Micromeritics, Autochem Z910). The standard procedure for TPD measurements involved the activation of the sample in flowing He at 873 K (3 h), cooling to 298 K, and adsorbing NH_3 from a stream of He–NH_3 (10%), removing the physically adsorbed NH_3 by desorbing in He at 373 K for 1 h, and finally carrying out the TPD experiment by raising the temperature of the catalyst in a programmed manner (10 K min^{-1}). The TPD curves were deconvoluted into two peaks, and the areas under the peaks were converted into meq NH_3 per gram of catalyst based on injection of known volumes of the He–NH_3 mixture under similar conditions. All of the samples were calcined at 823 K for 8 h prior to use in catalytic experiments.

APE (purity 99%) required for the reaction was synthesized by the reaction of allyl bromide and phenol in ethanol and purified by standard methods. The reactions were carried out in batch mode in a two-necked round-bottomed flask (capacity 25 ml) in a nitrogen atmosphere, with the use of 0.67 g of APE in 10 g of solvent (tetrachloroethylene, Loba Chemie) with 0.075 g of freshly calcined catalyst. Aliquots of the reaction mixture were collected at different time intervals and analyzed by gas chromatography (Varian gas chromatograph; column: CP Sil 5CB, 30 m; i.d. 0.05 mm; FID detector). The products were identified by gas chromatography-mass spectroscopy (GC-MS) and gas chromatography-infrared spectroscopy (GC-IR).

3. Results and discussion

3.1. Physicochemical characterization

3.1.1. X-ray diffraction

The XRD patterns of calcined Si- and Al-MCM-41 are shown in Fig. 1. The physicochemical properties of MCM-41 with different Si/Al ratios are presented in Table 1. The XRD patterns are similar to those reported for MCM-41 materials [9] and show low angle (110) and (200) peaks for all of the samples, which is characteristic of long-range order of crystallinity of the materials. Kresge et al. [9] indexed these peaks for a hexagonal unit cell, the parameter for which was calculated with the equation $a_0 = 2d_{100}/\sqrt{3}$ (Table 1). The table shows that the d_{100} reflection of Al-MCM-41 is shifted to higher values compared with its siliceous analogue. This is probably due to the framework substitution of Al in the MCM-41 structure [11]. The change in the T–O–T bond angle with Al substitution probably causes long-range disorder in the system and explains the slightly broader XRD peaks in Al-containing samples (Fig. 1).

3.1.2. Nuclear magnetic resonance

The ^{27}Al magic-angle spinning nuclear magnetic resonance (MAS NMR) spectrum of calcined Al-MCM-41 with

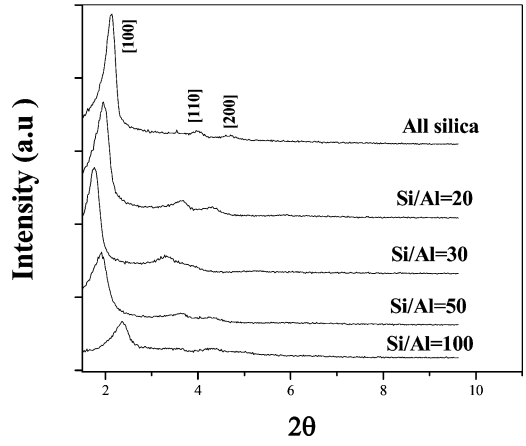

Fig. 1. XRD patterns of calcined Si-MCM-41 and Al-MCM-41 with different Si/Al ratios.

Table 1
Physicochemical properties of Al-MCM-41 samples

Sample	Si/Al ratio (XRF)	d_{100} spacing[a] (Å)	Unit cell a_0 parameter[a] (Å)	Surface area[b] (m^2/g)	Pore diameter[b] (Å)
Si-MCM-41	–	36.78	40.45	1094	28.58
Al-MCM-41 (100)	110.1	38.05	36.92	1219	27.23
Al-MCM-41 (50)	53.2	39.76	44.31	997	30.02
Al-MCM-41 (30)	31.0	40.49	44.38	873	31.44
Al-MCM-41 (20)	20.8	43.69	47.19	785	33.67

[a] As-synthesized sample.
[b] Calcined sample.

a Si/Al ratio of 20 is presented in Fig. 2. It reveals two peaks. The major peak, with a chemical shift of 52.52 ppm, is assigned to tetrahedrally coordinated Al presumably present in the Al-MCM-41 framework. The small peak at ∼ 0 ppm is due to octahedrally coordinated (nonframework) Al present in the material [12]. The spectrum shows that most of the Al in Al-MCM-41 is tetrahedrally coordinated, even at a high Al content (Si/Al = 20), and only a small amount of nonframework Al is present in the material.

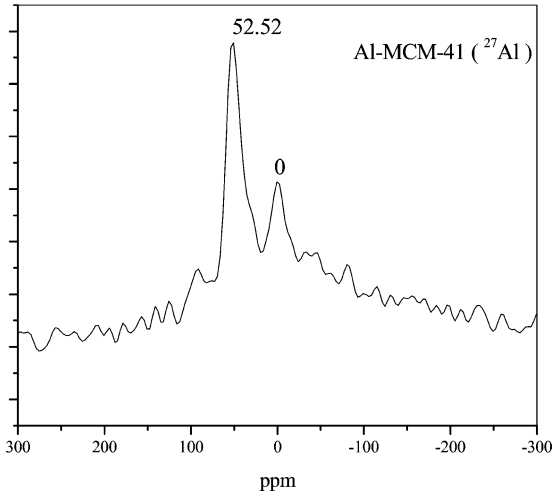

Fig. 2. ^{27}Al MAS-NMR spectrum of calcined Al-MCM-41 (Si/Al = 20).

3.1.3. Transmission electron microscopy

TEM images of calcined Al-MCM-41 (Si/Al = 50) and Si-MCM-41 revealed characteristic regular hexagonal arrays of uniform channels for both Al-MCM-41 (Si/Al = 50) and Si-MCM-41. The periodicity of the structure was also confirmed by the electron diffraction pattern.

3.1.4. Nitrogen sorption

The N_2 adsorption–desorption isotherms of MCM-41 and Al-MCM-41 were typical for type IV, with a hysteresis loop characteristic of mesoporous materials (Fig. 3). The isotherms exhibit three stages. The first stage is due to monolayer adsorption of nitrogen to the walls of the meso-

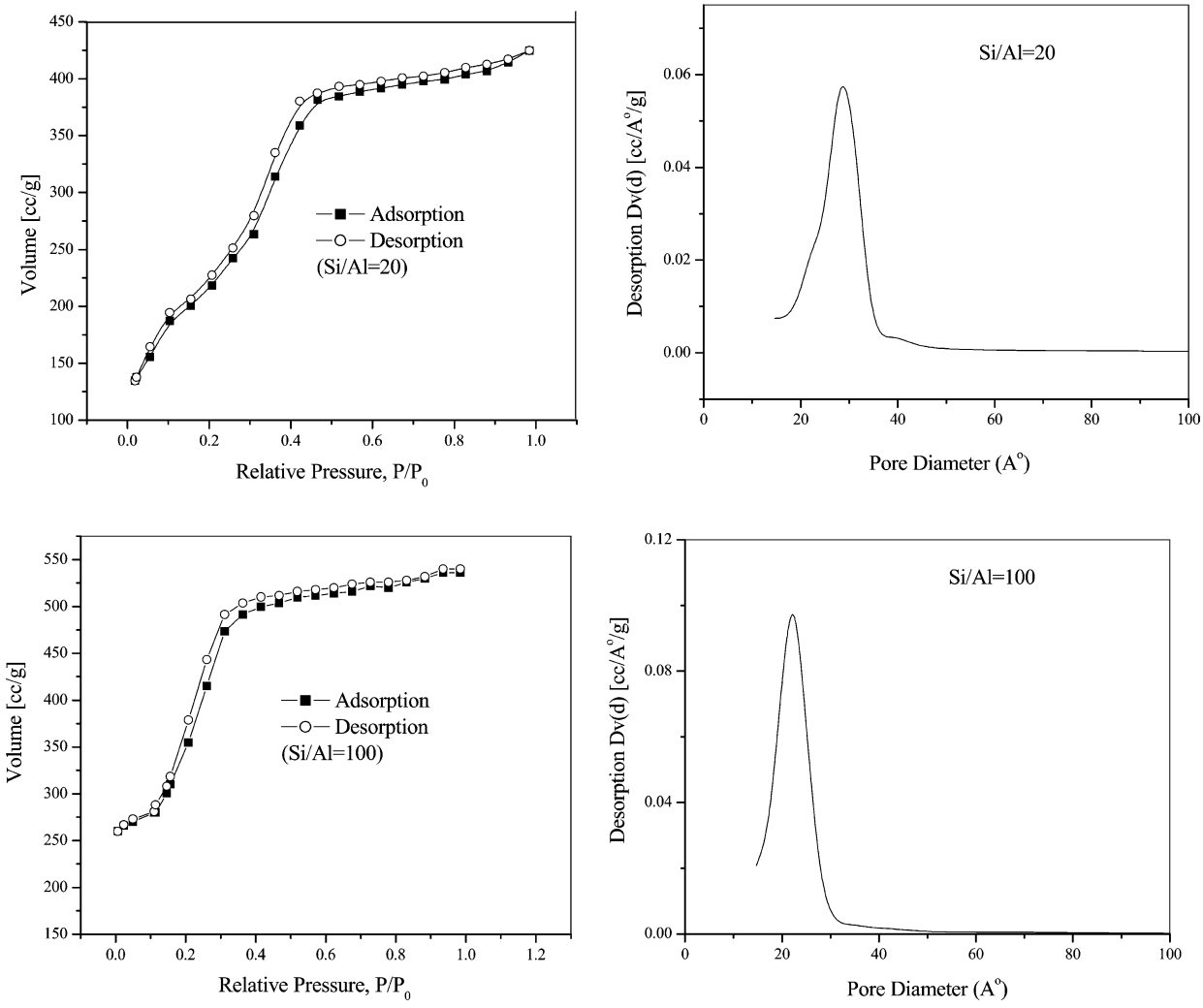

Fig. 3. Nitrogen adsorption isotherms and corresponding pore size distribution of calcined Al-MCM-41 with Si/Al ratios at 20 and 100.

pores at a low relative pressure ($p/p_0 < 0.2$). The second stage is characterized by a steep increase in adsorption ($p/p_0 > 0.2$). As the relative pressure increases, the isotherm exhibits a sharp inflection characteristic of capillary condensation within the uniform mesopores. The p/p_0 at the inflection is related to the diameter of the mesopore [13], and the steepness of this step indicates the uniformity of pore size distribution. The third stage in the adsorption isotherm is the gradual increase in volume with p/p_0 due to multilayer adsorption on the outer surface of the particles.

The surface area and average pore diameters of MCM-41 with different Si/Al ratios are given in Table 1. The table shows that the pore diameter increases with increasing Al content. The surface area decreases in general with increasing Al content in MCM-41, except in the case of the sample with Si/Al = 100, which shows a higher S_{BET} value. The reason for the anomalous behavior of the sample could be the poor crystallinity of the sample (XRD; Fig. 1).

The pore size distribution of calcined MCM-41 with Si/Al = 20 and 100 is also presented in Fig. 3. The figure shows that the materials possess pores of nearly uniform size with a narrow distribution. However, the distribution becomes broader as the Al content increases, because of the greater disorder caused by Al incorporation.

3.1.5. Temperature-programmed desorption of ammonia

The TPD profiles of Al-MCM-41 with different Si/Al ratios are presented in Fig. 4. The number and density of acid sites are expected to increase with the Al content [14]. Fig. 4 shows that the total acidity of MCM-41 increases with the Al content. The amounts of strong and weak acid sites in Al-MCM-41 with different Si/Al ratios, estimated from the deconvoluted TPD profiles, are given in Table 2. The table shows that the total number of acid sites (the strong and the weak acid sites) increases with Al content. The ratio of strong acid sites to weak acid sites also increases with Al content. Strong acid sites (Brønsted) are generated by tetrahedrally coordinated Al atoms forming Al–O(H)–Si bridges. The increase in the ratio of strong to weak acid sites with Al content implies that most of the added Al is tetrahedrally coordinated in the framework. Assuming that the strong acid sites are directly related to the Al ions in the samples, the ratio NH_3/Al (mole NH_3 desorbed per mole Al) was calculated (Table 2). The results indicate an increase in the ratio with decreasing Al content, suggesting an increasing dispersion of Al at higher Si/Al ratios.

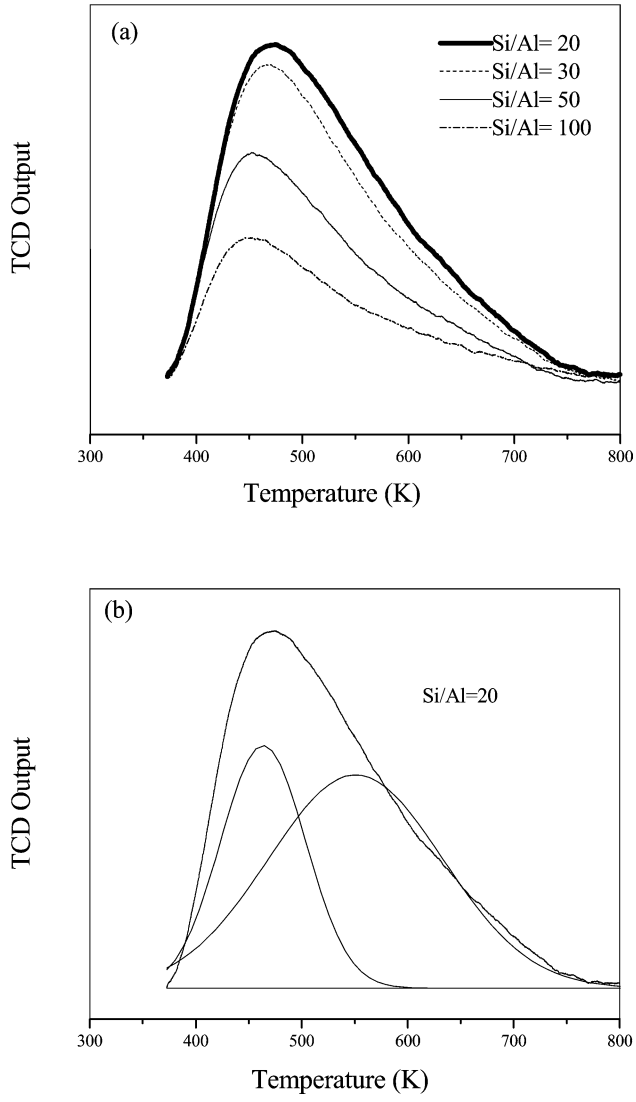

Fig. 4. (a) Temperature programmed desorption of ammonia from Al-MCM-41 with different Si/Al ratios. (b) Typical deconvoluted plot for sample with Si/Al = 20.

Table 2
Acidity of Al-MCM-41 with different Si/Al ratios by TPDA

Sample	Weak acidity (mmol/g)	Strong acidity (mmol/g)	Total acidity (mmol/g)	NH_3/Al[a] (mmol/g)
Al-MCM-41 (20)	0.098	0.152	0.250	0.20
Al-MCM-41 (30)	0.091	0.134	0.225	0.26
Al-MCM-41 (50)	0.064	0.093	0.157	0.30
Al-MCM-41 (100)	0.042	0.058	0.100	0.39

[a] Moles of NH_3 desorbed/mol of Al in the sample; based on NH_3 from strong acid sites.

3.2. Reaction studies

3.2.1. Claisen rearrangement of allyl phenyl ether

The catalytic activity of the calcined MCM-41 samples with different Si/Al ratios was compared for the Claisen rearrangement of APE. The reaction scheme is shown in Fig. 5. The ether first undergoes rearrangement to produce *o*-allylphenol (*o*-AP), which cyclizes to give 2,3-dihydro-2-methyl benzofuran (benzofuran).

3.2.1.1. Influence of duration of run The effect of run duration (up to 12 h) on conversion and on *o*-AP and benzofuran selectivities over the catalysts (with different Si/Al

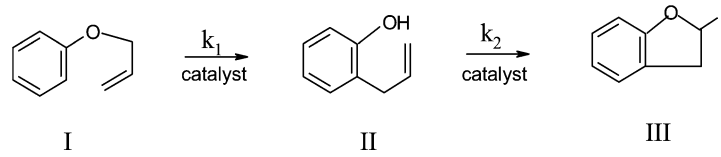

Fig. 5. Reaction scheme of Claisen rearrangement of allyl phenyl ether: **I**, allyl phenyl ether; **II** *o*-allylphenol; and **III**, 2,3-dihydro-2-methylbenzofuran.

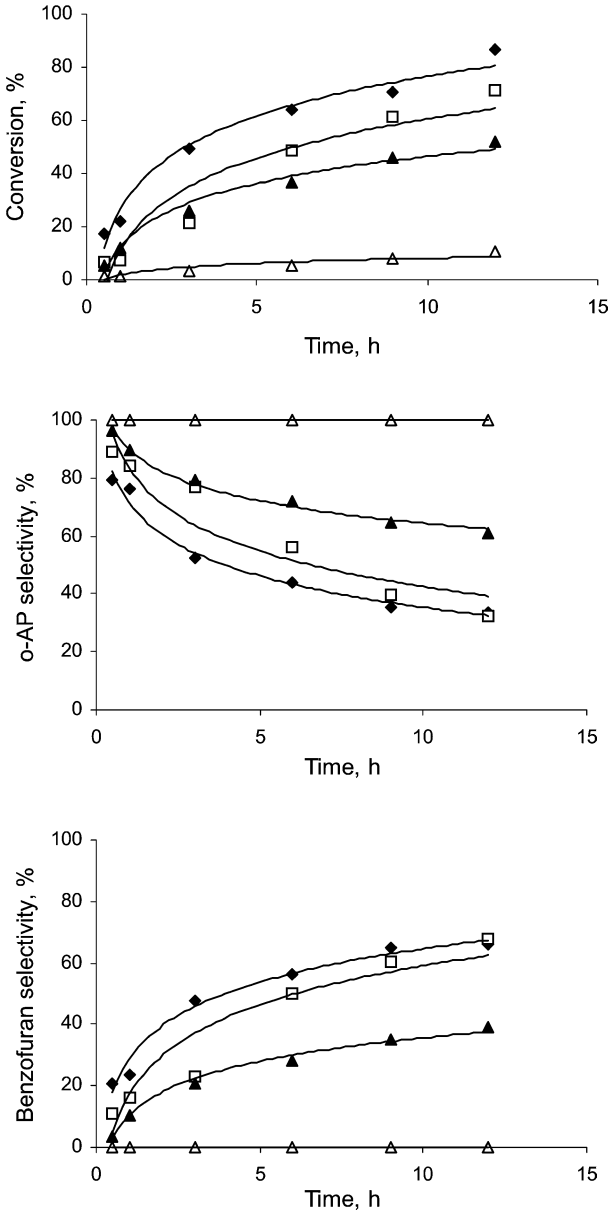

Fig. 6. Influence of Si/Al ratio and duration of run on the conversion and selectivity (reaction temperature, 393 K; ◆, Si/Al 20; □, Si/Al 30; ▲, Si/Al 50; △, Si/Al 100).

ratios) at 393 K are shown in Fig. 6. In general, the conversion and benzofuran formation increase with duration of run, whereas *o*-AP decreases. The activity increases with increasing Al content; the sample with the largest Si/Al ratio (∼ 100) is the least active.

3.2.1.2. Influence of temperature The influence of temperature on APE conversion and the *o*-AP and benzofuran selectivities for the samples with different Si/Al ratios are presented in Fig. 7. Conversion and ring formation increase with temperature for all Si/Al ratios, though the effect is less noticed for the most siliceous sample (Si/Al ∼ 100). *o*-AP selectivity increases with increasing Si/Al ratio and decreasing temperature; the influence of temperature is less at higher Si/Al ratios.

3.2.1.3. Influence of Si/Al ratio Both conversion and selectivity in the Claisen rearrangement are found to be dependent on the Si/Al ratio of MCM-41. Purely siliceous (Al-free) MCM-41 exhibited negligible conversion. Fig. 8 shows the influence of the Si/Al ratio on the reaction at different temperatures. The APE conversion decreases with decreasing aluminum content (increase in the Si/Al ratio) of the catalyst. The figure shows that a maximum conversion of up to 86.7% can be obtained with Al-MCM-41 with a Si/Al ratio of 20 at 393 K at the end of a 12-h reaction. The selectivity for *o*-AP increases and that for benzofuran decreases with an increasing Si/Al ratio in Al-MCM-41. As the reaction is catalyzed by the acid sites of Al-MCM-41, the observed behavior must be due to the decrease in the acidity of Al-MCM-41 with increasing Si/Al ratio (Table 2).

A plot of APE conversion and acidity (strong and weak) versus Al content is shown in Fig. 9a. It is found that both acidity and conversion increase with Al content. The close relationship between acidity and conversion suggests that the reaction occurs inside the pores of MCM-41. In the case of zeolites, however, the reaction was assumed to occur mainly on the external surface or at the pore mouth, as no relation between acidity (or Al content) and conversion was noticed [8].

The turnover frequency (TOF, mole of APE converted or product formed per hour per mole of Al present in the sample) is found to decrease with increasing Al content (for the samples with Si/Al ≈ 20, 30, and 50) (Fig. 9b). The data for the sample with Si/Al ≈ 100 do not fall in the above trend because of an unexpectedly small TOF, suggesting the nonaccessibility of the acid sites to the reactant molecules at low Al contents. On the other hand, a small increase in the TOF is noticed with increasing Al content for benzofuran formation. When the TOF (conversion of APE or formation of *o*-AP) is calculated based on the total number of acid sites (moles of NH_3 desorbed) in the three samples (Si/Al ≈ 20, 30, and 50), a nearly constant value (TOF = 8 ± 1 mol/(mol_{NH_3} h)) is obtained, revealing a direct relationship between acidity and activity in these samples.

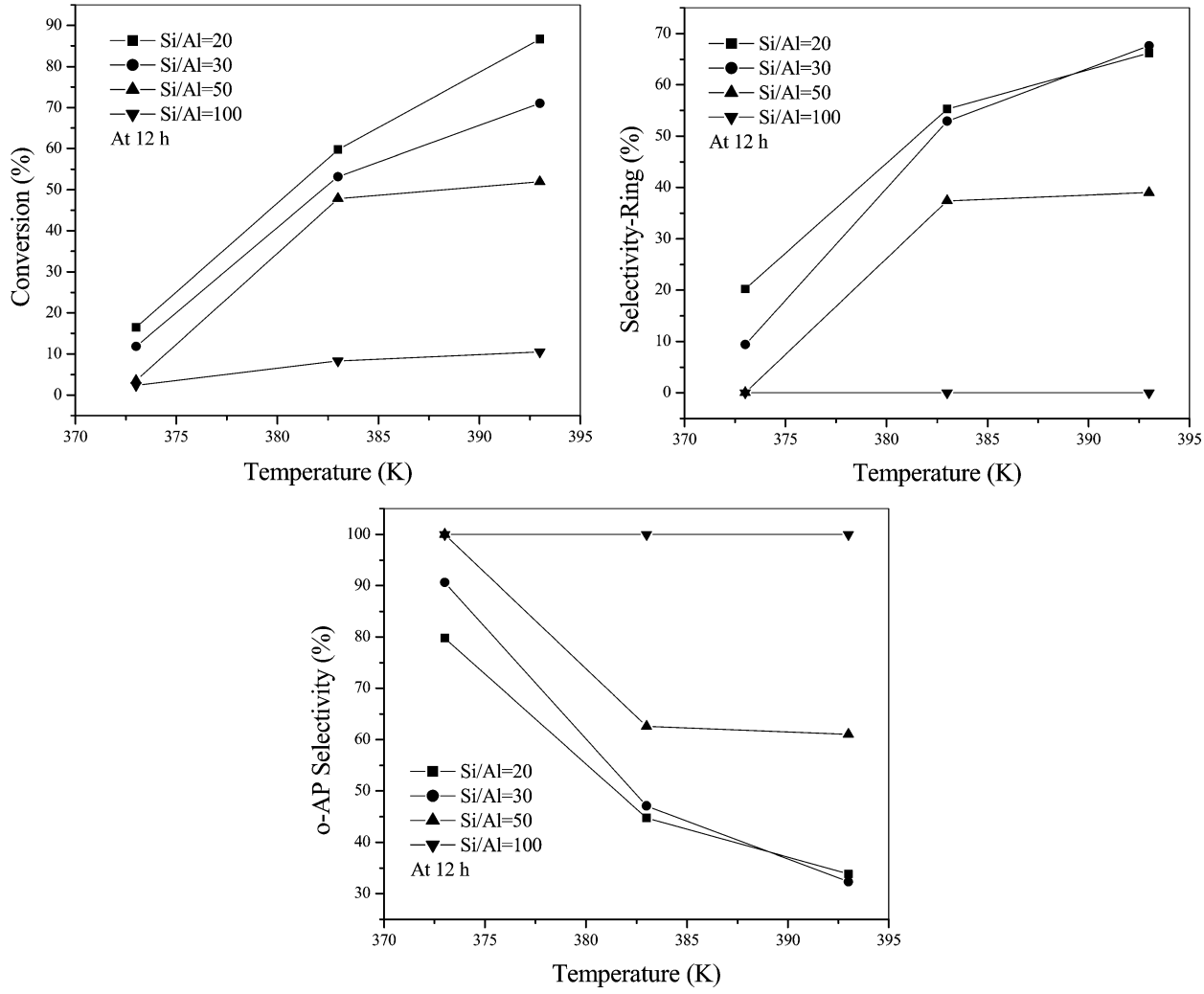

Fig. 7. Influence of temperature on conversion and selectivity over Al-MCM-41 with different Si/Al ratios.

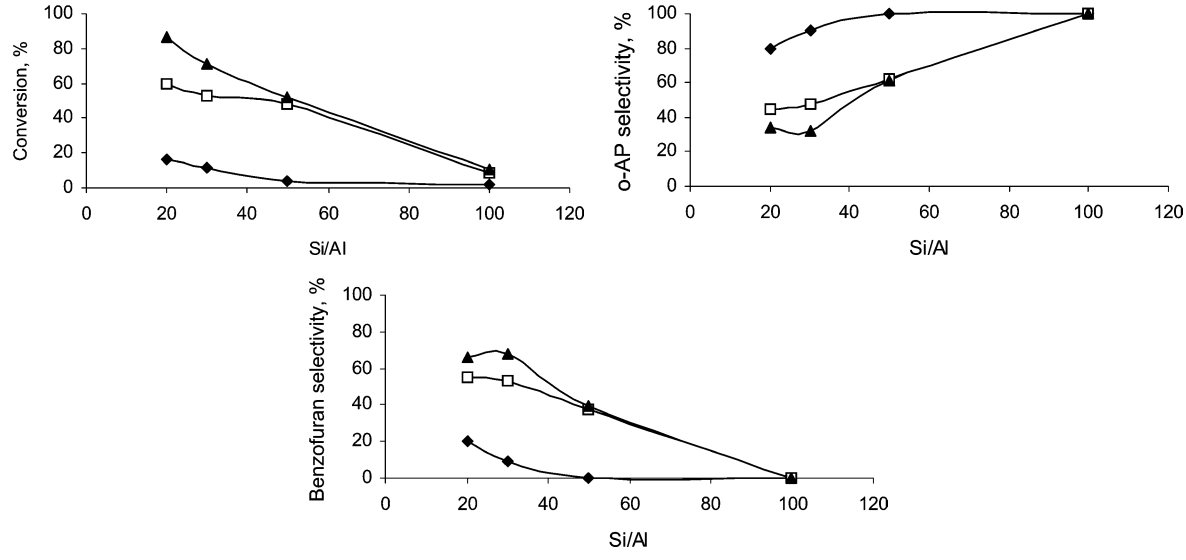

Fig. 8. Influence of Si/Al ratio on conversion and selectivity at different temperatures (reaction time, 12 h; ◆, 373 K; □, 383 K; ▲, 393 K).

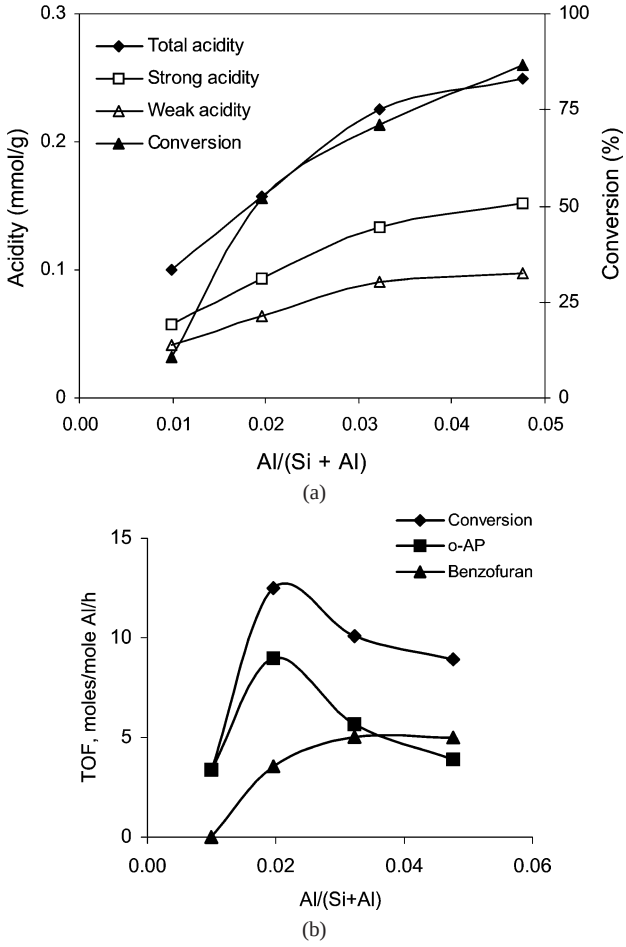

Fig. 9. Influence of Al-content on (a) APE conversion and catalyst acidity and (b) on TOF (reaction temperature, 393 K; time, 12 h).

3.2.1.4. Mechanism of the reactions A plausible mechanism for production by the Claisen rearrangement of the allyl phenol and its subsequent conversion to the ring compound is presented in Figs. 10a and b. The steps are catalyzed by acid centers. First the acid site protonates the oxygen of the ether. This is followed by intramolecular rearrangement of the protonated (adsorbed) species into the *o*-allylphenol as shown in Fig. 10a. The allyl phenol is next protonated at the allylic double bond to produce the secondary carbenium ion that reacts again intramolecularly with the phenolic oxygen to produce the benzofuran (Fig. 10b).

3.2.1.5. Kinetic analysis The scheme presented in Fig. 5 shows that the reaction involves two consecutive steps for the formation of benzofuran. Hence this was treated as a first-order series reaction with *o*-AP as the intermediate product, and the standard equations for a first-order series reaction were used for the determination of rate constants. These are

$$C_A/C_{A_0} = e^{-k_1 t} \quad (1)$$

and

$$C_R/C_{A_0} = k_1(e^{-k_1 t} - e^{-k_2 t})/(k_2 - k_1). \quad (2)$$

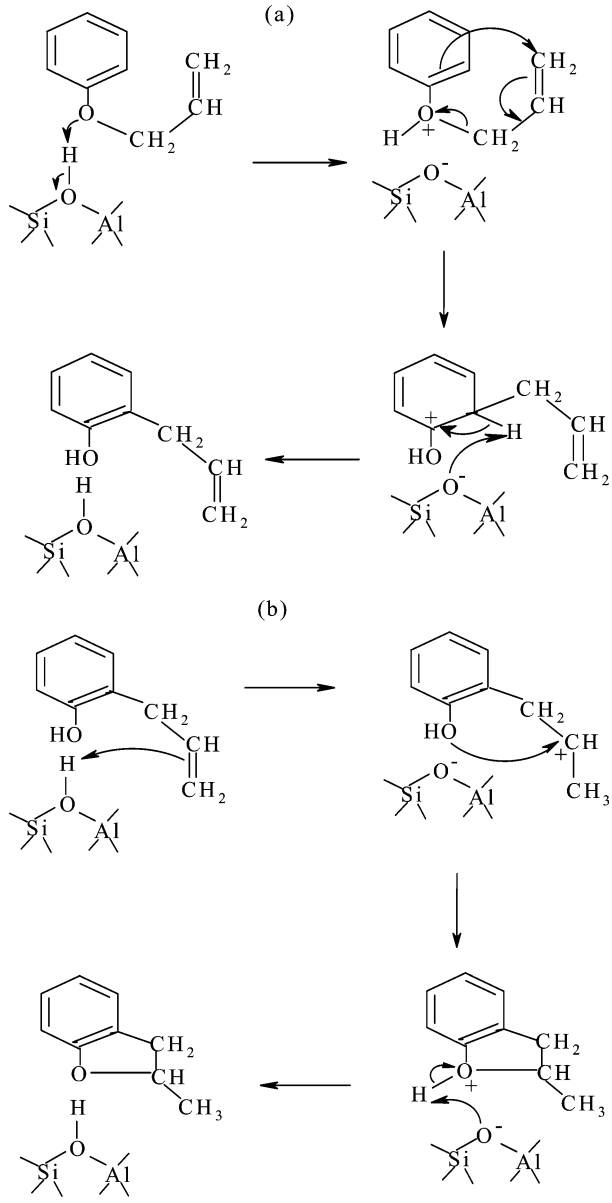

Fig. 10. Plausible mechanism of Claisen rearrangement of APE over solid acids (Al-MCM-41), for the formation: (a) of *o*-AP and (b) of ring product.

In the above equations, C_{A_0} and C_A are the concentrations of APE at initial time and at time t, respectively; C_R is the concentration of the intermediate product *o*-AP at time t; and k_1 and k_2 are the rate constants for the first and second steps, respectively.

The concentration profiles of APE, *o*-AP, and benzofuran for two temperatures (383 and 393 K) and Si/Al ratios (Si/Al = 20 and 30) in the Claisen rearrangement of APE are presented in Fig. 11. The lines represent the theoretical profiles. The profiles are those expected for typical first-order consecutive reactions. The nature of the profile, especially that for *o*-AP, depends on the relative values of k_1 and k_2. The rate equations and the time t_{max}, at which the intermediate *o*-AP concentration is maximum, are presented in Table 3. It can be seen from the table that t_{max}

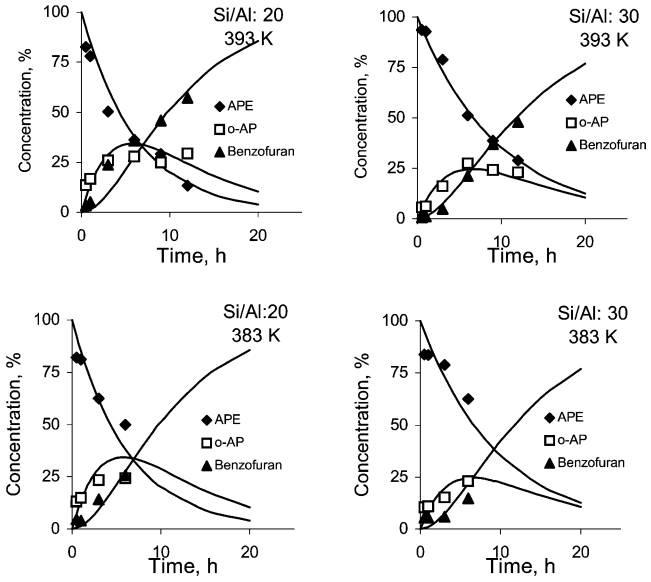

Fig. 11. Parity plots for the Claisen rearrangement of allyl phenyl ether at two different Si/Al ratios and temperatures. Experimental values are presented by symbols; bold lines represent profiles based on generated equations.

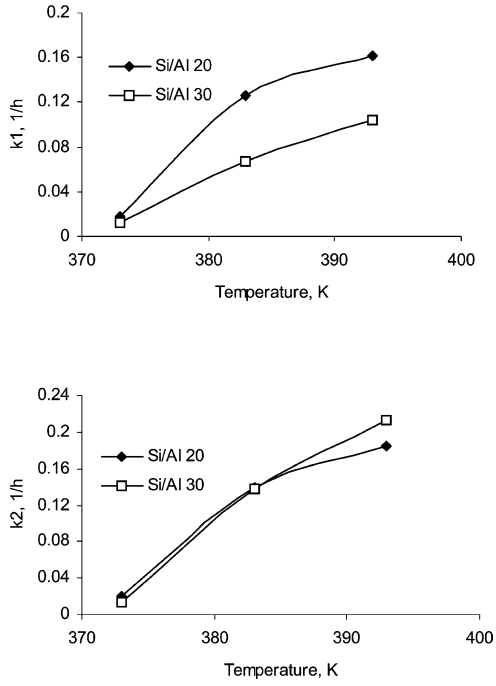

Fig. 12. Influence of temperature and Si/Al ratio on the reaction rate constants.

varies with both the reaction temperature and the Si/Al ratio of MCM-41. For a given catalyst, t_{max} decreases with increasing temperature and Al content.

The influence of temperature and Si/Al ratio (20 and 30) on the reaction rate constants, k_1 and k_2, is presented in Fig. 12. The figure shows that both k_1 and k_2 increase with increasing temperature. It is found that k_2 is not much affected by variation in the Si/Al ratio, whereas k_1 is sensitive. The reasons for this are not clear.

The activation energy for the two steps was calculated with the Arrhenius expression. The activation energy for the reaction of APE on Al-MCM-41 with a Si/Al ratio of 20 is estimated to be 8.9 kcal/mol. The activation energy for the formation of benzofuran from *o*-AP is estimated to be 10.3 kcal/mol. The activation energy of the reactions was not found to be significantly affected by a change in the Si/Al ratio.

4. Conclusions

The Claisen rearrangement of APE over Al-MCM-41 proceeds with ease in tetrachloroethane. *o*-Allyl phenol is produced initially, which then undergoes cyclization to form 2,3-dihydro-2-methylbenzofuran. The reaction takes place on the acid sites of the catalyst. Both the catalyst acidity and substrate conversion increase with the Al content in MCM-41. There is a close relationship between acidity and conversion, which suggests that the reaction occurs inside the pores of MCM-41. The conversion and benzofuran formation increase with run duration, whereas the *o*-AP decreases, as expected for a consecutive reaction. The temperature effects on conversion and selectivity are more pronounced at low Si/Al ratios than at high Si/Al ratios. *o*-AP selectivity increases with increasing Si/Al ratio and decreasing temperature. The reaction kinetics was analyzed under the assumption that it is

Table 3
Results of kinetic analysis for Al-MCM-41 catalysts with Si/Al = 20 and 30

Si/Al	T[a]	Rate constants		Rate expressions		t_{max}[c]
	(K)	k_1 (1/h)	k_2 (1/h)	Eq. (1)[b]	Eq. (2)[b]	(h)
20	383	0.13	0.14	$C_A/C_{A_0} = e^{-0.13t}$	$C_R/C_{A_0} = 0.13(e^{-0.13t} - e^{-0.14t})/0.01$	7.55
	393	0.16	0.18	$C_A/C_{A_0} = e^{-0.16t}$	$C_R/C_{A_0} = 0.16(e^{-0.16t} - e^{-0.18t})/0.02$	5.80
30	383	0.07	0.14	$C_A/C_{A_0} = e^{-0.07t}$	$C_R/C_{A_0} = 0.07(e^{-0.07t} - e^{-0.14t})/0.07$	10.18
	393	0.10	0.21	$C_A/C_{A_0} = e^{-0.10t}$	$C_R/C_{A_0} = 0.10(e^{-0.10t} - e^{-0.21t})/0.11$	6.58

[a] Reaction temperature.
[b] See text, kinetic analysis.
[c] The time at which the concentration of *o*-AP reaches a maximum value.

a first-order consecutive reaction. On Al-MCM-41, both k_1 and k_2 increase with increasing temperature. k_2 is not much affected by variation in the Si/Al ratio, whereas k_1 is sensitive. The time at which the intermediate *o*-AP concentration is maximum, t_{max}, varies with both the reaction temperature and the Si/Al ratio of MCM-41. For a given catalyst, t_{max} decreases with increasing temperature and Al content.

References

[1] J. March, Advanced Organic Chemistry, fourth ed., Wiley, New York, 1992.
[2] R.P. Lutz, Chem. Rev. 84 (1984) 205.
[3] K. Pitchumani, M. Warrier, V. Ramamurthy, J. Am. Chem. Soc. 118 (1996) 9428.
[4] J.A. Elings, R.S. Downing, R.A. Sheldon, Stud. Surf. Sci. Catal. 94 (1995) 487.
[5] R.A. Sheldon, J.A. Elings, S.K. Lee, H.E.B. Lempers, R.S. Downing, J. Mol. Catal. A: Chem. 134 (1998) 129.
[6] I. Sucholeiki, M.R. Pavia, C.T. Kresge, S.B. Mc Cullen, A. Malek, S. Schram, Mol. Divers. 3 (1998) 151, CA: 129: 202736 (1999).
[7] R. Cruz-Almanza, F. Perez-Flores, L. Brena, E. Tapia, R. Ojeda, A.J. Fuentes, Heterocycl. Chem. 32 (1995) 219.
[8] S.G. Wagholikar, S. Mayadevi, S.P. Mirajkar, S. Sivasanker, in: E. van Steen, L. Callanan, M. Claeys, C.T. O'Connor (Eds.), Proceedings of 14th International Zeolite Conference, Cape Town, 2004, p. 2731.
[9] C.T. Kresge, M.E. Leonowicz, W.J. Roth, J.C. Vartuli, J.S. Beck, Nature 359 (1992) 710.
[10] J.S. Beck, J.C. Vartuli, W.J. Roth, M.E. Leonowicz, C.T. Kresge, K.D. Schmitt, C.T.W. Chu, D.H. Olson, E.W. Scheppard, S.B. MacCullen, H.B. Higgins, J.L. Schlenker, J. Am. Chem. Soc. 114 (1994) 10834.
[11] R.B. Borade, A. Clearfield, Catal. Lett. 31 (1995) 267.
[12] X. Chen, L. Huang, G. Ding, Q. Li, Catal. Lett. 44 (1997) 123.
[13] S.J. Gregg, K.S.W. Suig, Adsorption, Surface Area and Porosity, Academic Press, London, 1982, Ch. 4.
[14] H. Kosslick, G. Lischke, B. Parlitz, W. Storek, R. Fricke, Appl. Catal. A. Gen. 184 (1999) 49.